EUROPEAN MATERIALS RESEARCH SOCIETY
E-MRS

SOLID STATE IONICS

Edited by

Minko BALKANSKI

Laboratoire de Physique des Solides
Université Pierre et Marie Curie
4 place Jussieu
75252 Paris Cedex 05, France

and

Claude DELMAS

Laboratoire de Chimie du Solide du CNRS
Université de Bordeaux I
251 Cours de la Libération
33405 Talence Cedex, France

June 1991

VIBRATIONAL STRUCTURAL STUDIES OF ALKALI BORATE GLASSES

E.I.Kamitsos and G.D.Chryssikos
Theoretical and Physical Chemistry Institute
National Hellenic Research Foundation
48, Vass. Constantinou Ave., Athens 116 35
Greece

1. INTRODUCTION

Binary alkali borate glasses $xM_2O(1-x)B_2O_3$ (M=alkali) have been extensively studied over the years to elucidate the nature and the relative concentration of the various borate units constituting the glass network. The ultimate goal was to understand the structural peculiarities of these materials, which are manifested by the non-monotonic variation of most physical properties with x and are widely known as the "boron anomaly effect"(1). The NMR investigation of Bray et al (2,3) as well as the vibrational work of Krogh-Moe (4) and Konijnendijk and Stevels (5) were particularly helpful in identifying various boron-oxygen arrangements at different modification levels. These studies have put emphasis on the effect of modifier content (x) on the glass structure, but provided little or no insight in the possible dependence of the latter on the nature of the particular alkali employed.

Interest in structural studies of borate glasses has been renewed since the discovery of glass compositions with exceptionally high ionic conductivity, which are promissing for energy storage and microionics applications (6). In that respect, binary alkali borate glasses are of special interest since they can be good ionic conductors by themselves (7,8) and /or form the basis of multicomponent fast ionic conductors (6,9-11). Enhanced ionic conductivity is usually related to

high contents of metal oxide modifier in both binary and multicomponent systems (9,10).

It has been recognized that the limited structural understanding of glasses, inherent to their disordered nature, is the main reason for the lack of a comprehensive theory for the ion transport mechanism in amorphous solids (9, 10,12). Previous vibrational studies of alkali borate glasses have been limited to compositions with rather low M_2O contents ($x<0.40$). Since most of the current interest is focussed on glasses with high M_2O concentrations, it has been desirable to extend these studies to such materials.

In this report, we compile representative Raman spectra of sodium- and caesium-borate glasses, with compositions covering a continuous and very broad glass forming range ($0 \leq x \leq 0.75$). These spectra will enable the systematic study of the variation of the glass network structure with metal oxide content. In addition, Raman spectra of borate glasses with fixed M_2O content will be presented to illustrate the alkali cation effect on the glass structure.

The thorough understanding of the vibrational characteristics of glassy materials has required the parallel study in the infrared (13) because of the complementarity of selection rules. Most of the older infrared studies on borate glasses have been performed on low-M_2O content samples dispersed in a variety of media and cover independently the mid- (4,, 14-17) and far-infrared (18, 19) spectral regions. Some reflectance investigations have also been reported but most of them are limited to the mid-infrared range (20-22). By taking advantage of the capabilities of the modern Fourier-transform spectrometers infrared reflectance data on a wide frequency range (30-4000 cm^{-1}) have been recently acquired in our laboratory. Thus, the simultaneous study of both, the glass network structure in the mid-infrared and the cation-network interactions active in the far-infrared, is now possible. Spectra of characteristic compositions in the system $xLi_2O.\ (1-x)B_2O_3$ ($0 \leq x \leq 0.73$) are presented and discussed in relation to the Raman data.

2. GLASS PREPARATION

Binary alkali borate glasses are usually prepared from reagent grade powders of anhydrous B_2O_3 and dried metal carbonates, mixed in appropriate amounts and melted in Pt crucibles . Small replacement of B_2O_3 by Al_2O_3 (~5 mol%) is necessary to ensure the glass formability of sodium, potassium and rubidium borate glasses with $0.45 \leq x \leq 0.55$ (23,24). Melting times of ca 10-30 min, and temperatures in the range 800-1200 ^{o}C, depending on composition, are appropriate to obtain clear and bubble-free melts. Glassy samples can then be prepared by quenching the melt between two copper blocks. An updated version of the alkali borate glass forming regions is shown in Figure 1 for reference.

Samples containing small, ($x<0.15$), or large, ($x>0.50$) amounts of alkali metal oxide are hygroscopic, and thus special care is needed to avoid hydrolysis Some carbonate retention can not be avoided in high M_2O content glasses due to their high melt basicity (23,24). Further details on sample preparation and handling can be found elsewhere (14, 25,26).

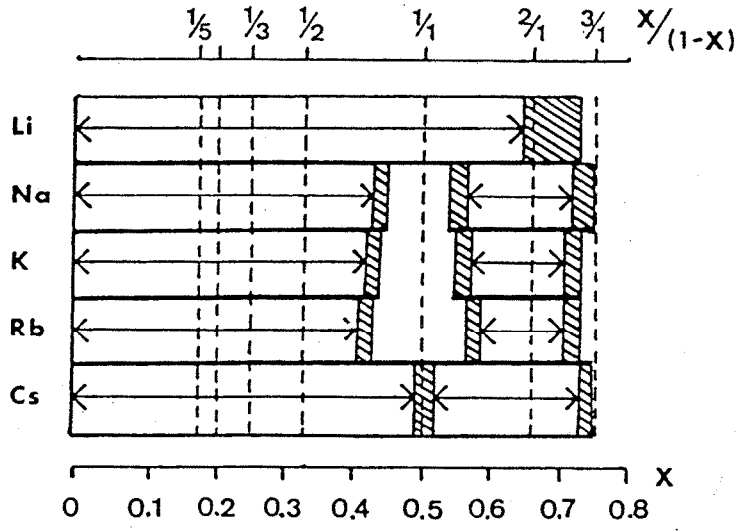

Figure 1. Glass forming regions of alkali borate glasses. Shaded areas indicate vitrification of small batches by splat or roller quenching. Vertical lines indicate cystalline borate stoichiometries.

3. RAMAN SPECTRA OF ALKALI BORATE GLASSES

3.1 The Structure of Sodium- and Caesium-Borate Glasses over Extended Composition Ranges.

The Raman spectra of sodium-borate glasses are shown in Figure 2 for several compositions with relatively low Na_2O content. The spectrum of glassy B_2O_3 (x=0) is characterized by the strong, sharp and highly polarized band at 806 cm^{-1}. The origin of this band has been the subject of extensive investigations, which have led to its, quite well accepted by now , assignment to the symmetric ring breathing vibration of the boroxol ring (Figure 3(1)) (27-32).

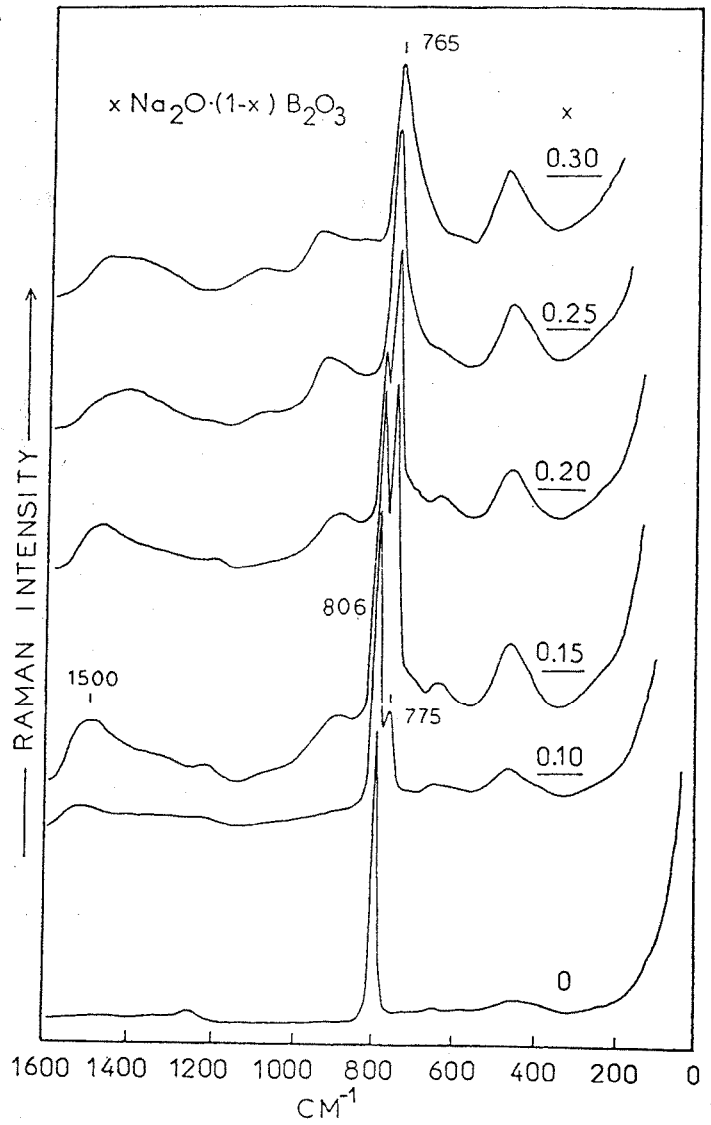

Figure 2. Raman spectra of sodium-borate glasses, $xNa_2O.(1-x)B_2O_3$, in the composition range: $0 \leq x \leq 0.30$.

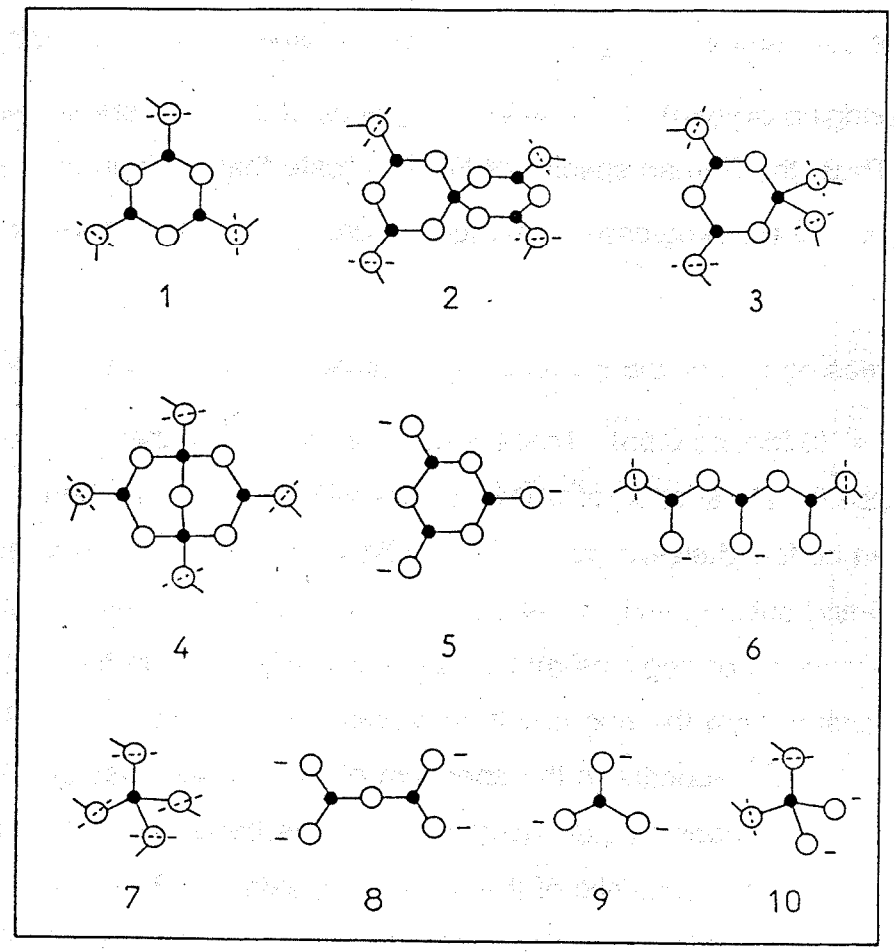

Figure 3. Structural groups postulated for borate glasses: (1) boroxol ring, (2) pentaborate unit, (3) triborate unit, (4) diborate unit, (5) metaborate ring, (6) metaborate chain, (7) "loose" $B\emptyset_4^-$ tetrahedron, (8) pyroborate unit, (9) orthoborate unit and (10) boron-oxygen tetrahedron with two bridging and two non-bridging oxygens. Solid circles represent boron atoms, open circles oxygen atoms. Note that O with a slash indicates a bridging oxygen and O^- indicates a non-bridging oxygen.

Addition of Na_2O to B_2O_3 appears to cause substantial structural changes in the borate network, evidenced by alterations in the Raman vibrational characteristics. The most important effect of increasing x is the rapid decrease of the 806 cm^{-1} band intensity, with the simultaneous development of a new band at ca 770 cm^{-1}. For the glass composition x=0.25 the 806 cm^{-1} feature has disappeared, indicating the absence of boroxol rings, while that at 765 cm^{-1} becomes the dominant Raman band. The latter feature has been observed in the spectra of similar glasses and assigned by Brill (33) to the symmetric ring breathing vi-

bration of six-membered ring arrangements containing one or two $B\emptyset_4^-$ tetrahedra (Ø=bridging oxygen). Several borate groups of this kind are shown in Figure 3(2,3). Thus, the Raman spectra of Fig.2 indicate that addition of sodium oxide to B_2O_3 cause the progressive change of boron coordination number from three to four.

Increasing further the Na_2O content causes drastic spectral effects, shown in Figure 4 ($0.35 \leq x \leq 0.55$). These Raman spectra are rather complex and only the compositional variation of a few bands will be discussed here, while more details can be found elsewhere (25). The band at 630 cm^{-1}, which appears first at x=0.35 and subsequently develops with x, is of particular interest since it indicates the creation of ring-type metaborate units (Fig.3(5)). In fact, the 630 cm^{-1} band originates from the ring breathing vibration of the latter units (33). A new band at 820 cm^{-1} appears in the spectrum of the x=0.45 glass and becomes a dominant feature upon further increasing x. This band, as well as the one at 1210 cm^{-1}, are characteristic of the pyroborate units (Fig.3(8)), originating from the symmetric stretching vibration of B-O-B bridges and terminal $B-O^-$ bonds respectively (25). Thus, the sequence of the Raman spectra presented in Figure 4 indicate that, for this particular composition range, addition of Na_2O results in a progressive disruption (i.e. depolymerization) of the borate network, through the formation of non-bridging oxygen-containing borate units. Such representative units are the metaborate rings and the pyroborates, both representing "molecular" type moieties which are completely dismantled from the covalent borate network.

Representative Raman spectra of Na-borate glasses with compositions $0.61 \leq x \leq 0.75$ are depicted in Figure 5. It is quite clear that the bands at 630, 755, 820 and 1210 cm^{-1}, as well as the ones at ca 550 and 940 cm^{-1}, suffer a systematic intensity decrease upon increasing x. Thus, the borate groups responsible for these bands are progressively destroyed in such high Na_2O-content borate glasses. This is accompanied by the appearance of the 895 cm^{-1} feature (x=0.61) which increases in intensity with x and eventually becomes the main band of the x=0.75 glass spectrum. This band is attributed to the symmet-

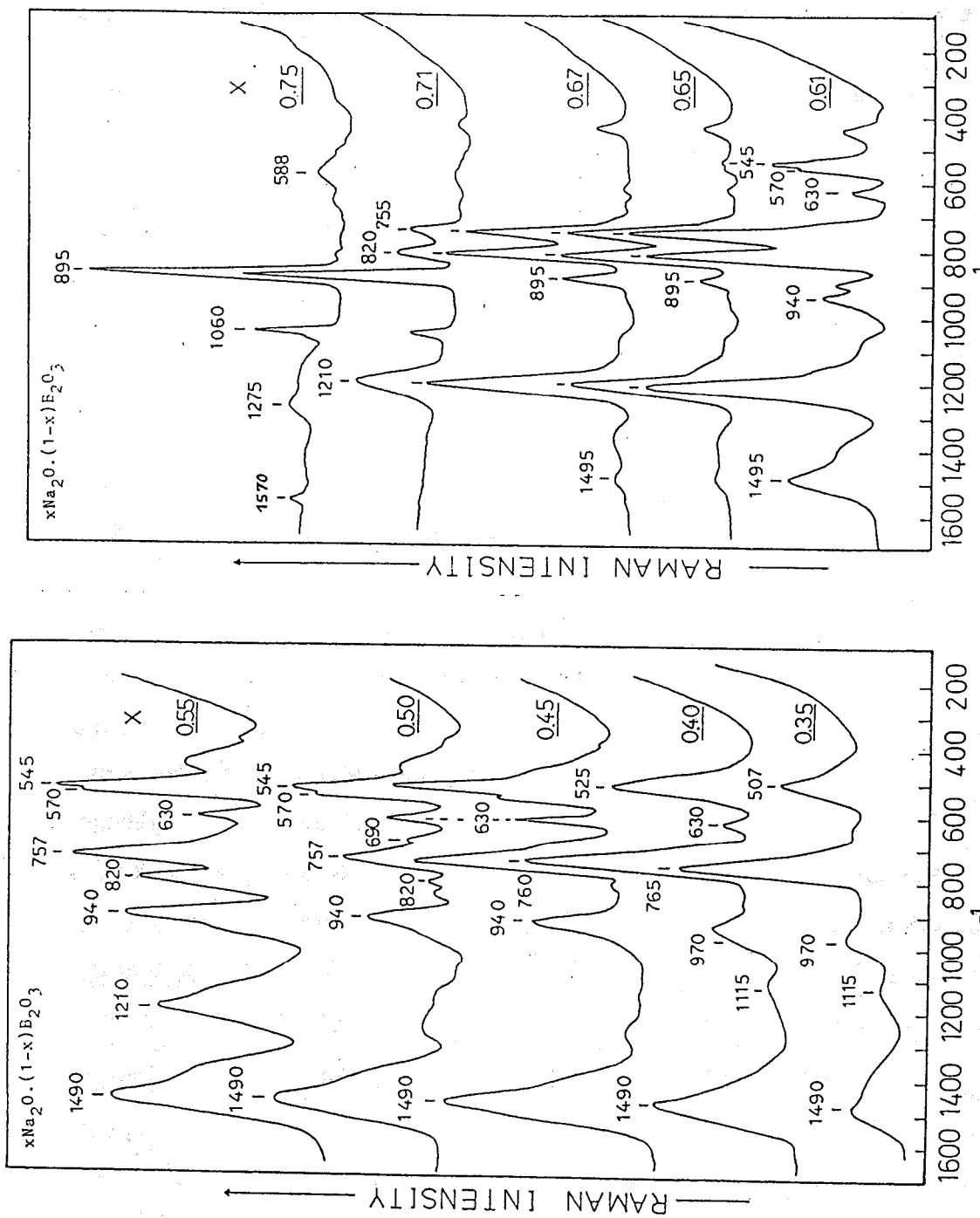

Figure 4. Raman spectra of $xNa_2O.(1-x)B_2O_3$ glasses in the composition range: $0.35 \leq x \leq 0.55$.

Figure 5. Raman spectra of $xNa_2O.(1-x)B_2O_3$ glasses in the composition range $0.61 \leq x \leq 0.75$.

ric stretching vibration of the planar orthoborate units, BO_3^{3-} (Fig. 3 (9)). In addition the weak band at 1275 cm^{-1} is assigned to the asymmetric stretching of BO_3^{3-}, while the one at 588 cm^{-1} to the in-plane bending mode of the same unit (25). The weak band observed at 1570 cm^{-1} can be assigned to the overtone of the out-of-plane bending mode of BO_3^{3-}, which is infrared active only at 780 cm^{-1} (34).

Besides the bands attributed to BO_3^{3-} species the spectrum of the x=0.75 glass exhibits a sharp band at 1060 cm^{-1}, which was assigned to the totally symmetric stretching vibration of carbonate species, CO_3^{2-} (35) These are present in such high basicity borate glasses and their influence on the glass structure, their interaction with the glassy environment, as well as their dependence on melting time, temperature and composition have been recently investigated (36).

The Raman spectra of Cs-borate glasses have also been reported for compositions in the range: $0 \leq x \leq 0.50$ (37). It was observed that for small values of x, the Cs-glass spectra are quite similar to the corresponding ones of Na-borate glasses. The cation dependence of the borate glass network is consequently rather small at low modification levels, but becomes progressively very significant as x increases towards the metaborate stoichiometry. Thus, the spectrum of the x=0.50 Cs-borate glass, (Figure 6),exhibits pronounced differences compared to that of the Na-glass of the same alkali content. It should be kept in mind that the spectrum of sodium metaborate is that of a pseudo-binary glass containing ca 5 mol % Al_2O_3. The alumina-free Na-melt is not glass-forming, contrary to the corresponding Cs-melt and this illustrates even better the role of the modifying cation in determining the structure of borate networks . This has triggered the extension of the glass forming region of the Cs_2O-B_2O_3 system (26) and the structural study the structure of the obtained glasses.

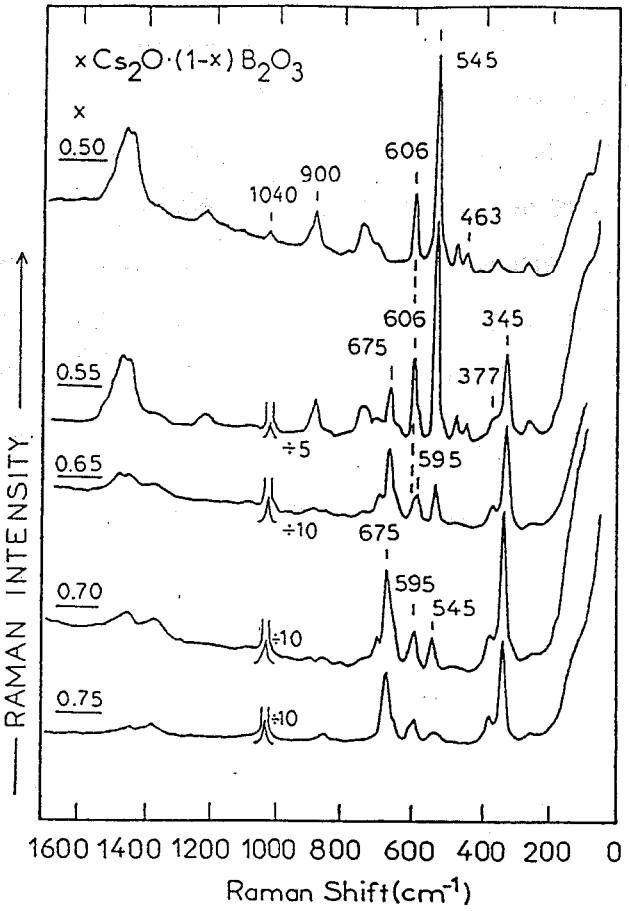

Figure 6. Raman spectra of $xCs_2O.(1-x)B_2O_3$ glasses ($0.50 \leq x \leq 0.75$).

The Raman spectrum of the Cs-metaborate is characterized by sharp bands at 606 and 545 cm^{-1} which have been attributed to metaborate rings and "loose" $B\emptyset_4^-$ tetrahedra, respectively (37). The former groups are also responsible for the 370, 463 and 1400-1600 cm^{-1} features. The latter units (Fig. 3(7)) are boron oxygen tetrahedra isomeric to the metaborate triangles $B\emptyset_2O^-$, and are thought to connect various segments of the glass network without participating to specific borate arrangements.The 900 cm^{-1} band was assigned to the asymmetric vibration of "loose" $B\emptyset_4^-$ tetrahedra, while that at 1040 cm^{-1} is indicative of the presence of some undissociated carbonates (37).

At higher Cs_2O contents all spectral features related to the aforementioned boron oxygen units appear to decrease in intensity, indicating that those units are

no longer favoured. Instead, the spectral activity is progressively enhanced around 675 cm^{-1} and 345 cm^{-1}. These features maintain fixed relative intensities regardless of the extend of their coexistence with bands that characterize the metaborate glass, and finally dominate the spectrum of the orthoborate composition (x=0.75). It was argued, on the basis of the similarity between the spectrum of the x=0.75 Cs- borate glass and those of calcium orthoaluminate and orthogallate, that the new features at 675, 377 and 345 cm^{-1} denote the existence of $B\emptyset_2O_2^{3-}$ units (Fig.3(10)) (26). These are boron oxygen tetrahedra with two bridging (Ø) and two non bridging (O^-) oxygen atoms.

The majority of crystalline orthoborate compounds are formed by isolated triangular orthoborate units, BO_3^{3-}, which were also found to constitute the 'network' of the x=0.75 Na-borate glass. However, such units are not present in the corresponding Cs-borate glass, but instead, they are replaced by their isomeric $B\emptyset_2O_2^{3-}$ species. Thus, it appears that the structure of the borate glass network is a function of both content and nature of the metal oxide present. The effect of the nature of alkali metal is examined in more detail in the following section.

3.2. Alkali Cation Dependence of the Borate Glass Structure

As noted above, differences between the spectra of alkali borate glasses of the same x value are mainly manifested at high alkali contents. Nevertheless, a careful examination of the Raman spectra of glasses with relatively low M_2O contents has also revealed the dependence of the network structure on the particular alkali employed (38). Figure 7 illustrates the Raman spectra of borate glasses with x=0.70. This particular composition lies roughly halfway between the pyroborate (x=0.67) and orthoborate (x=0.75) compositions, and thus it should in principle correspond structurally to a mixture of the corresponding isolated moieties (Fig. 3(8,9)). Indeed, the spectrum of the lithium glass exhibits bands characteristic of orthoborate (925 cm^{-1}) and pyroborate (835, 1250 cm^{-1}) units, as well as six membered rings with $B\emptyset_4^-$ tetrahedra (763 cm^{-1}). The

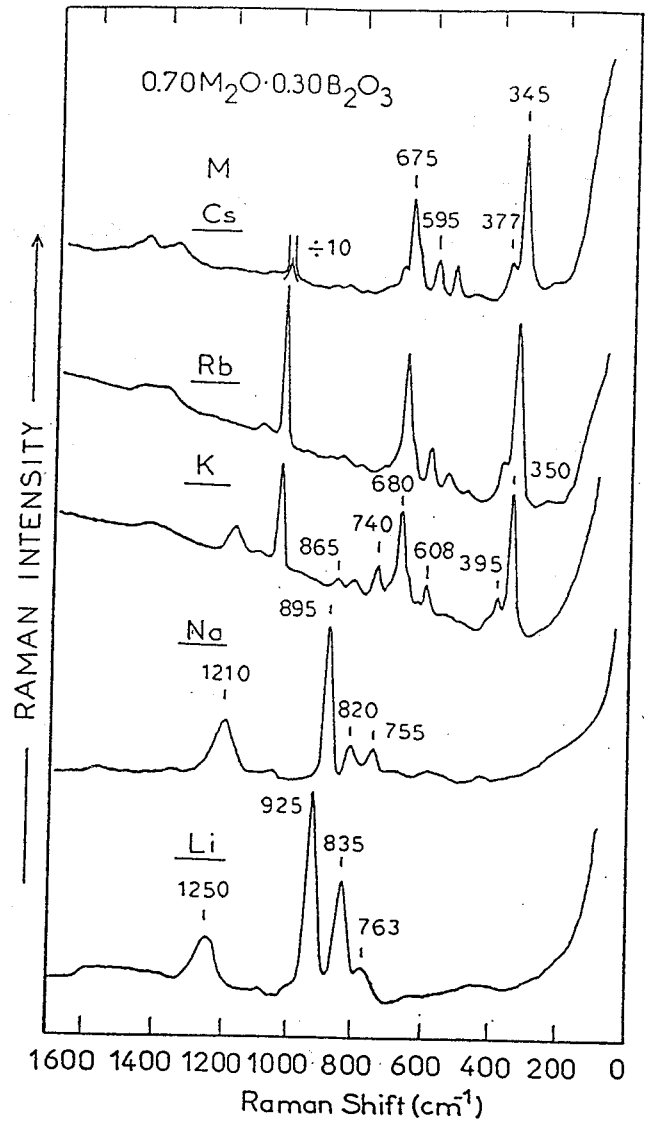

Figure 7. Raman spectra of alkali borate glasses of composition $0.70M_2O.\ 0.30B_2O_3$,

same network building units are evident in the spectrum of the corresponding Na glass. They are also present in the K-glass, as manifested by their corresponding Raman bands, which are now coexisting with a number of new features. For instance,we can deduce the presence of metaborate rings (608 cm^{-1}) and chains (740 cm^{-1}) in addition to orthoborate triangles (865 cm^{-1}) and pyroborates (810 and 1180 cm^{-1}) (37). The formation of $B\emptyset_2O_2^{3-}$ tetrahedra is also evident, on the basis of the presence of the 680, 395 and 350 cm^{-1} bands . These features grow mainly at the expense of the band characteristic of orthoborate triangles

(865 cm^{-1}), which has suffered a significant loss in relative intensity from Na to K. The spectra of the Rb-and Cs-glasses recover their simplicity in a way that bears no similarity with those of Li-and Na-glasses. Thus, the predominant network unit appears to be the four-coordinated $B\emptyset_2O_2^{3-}$ species (675, 377 and 345 cm^{-1}), while some "loose" $B\emptyset_4^-$ tetrahedra (545 cm^{-1}) and metaborate rings (~600 cm^{-1}) are also present.

On the basis of the Raman spectra, discussed above, glass formation of highly modified borate glasses seems to be associated with the existence of the following set of high temperature equilibria (26):

meta- : x=0.50, (BO_2^-) $\quad B\emptyset_2O^- \Leftrightarrow B\emptyset_4^-$ (1)

pyro- : x=0.67, ($BO_{2.5}^{2-}$) $\quad 2B\emptyset O_2^{2-} \Leftrightarrow (BO_3^{3-}) + (BO_2^-)$ (2)

ortho-: x=0.75, (BO_3^{3-}) $\quad BO_3^{3-} \Leftrightarrow B\emptyset_2O_2^{3-}$ (3)

It is obvious that the above equilibria are strongly cation dependent. For example, Eqs.(2) and (3) are shifted to the left for M=Li, Na. The K-analog, whose spectrum is the most complex of all, favours the coexistence of all reactants and products of Eqs.(1)-(3). In Rb- and Cs- glasses of high M_2O contents (x=0.70), the Raman spectra indicate that all three equilibria are shifted to the right, resulting in network tetrahedra with none and/or two non-bridging oxygens.

Freezing the above equilibria at the fictive temperature accounts for the observed diversity in borate glass structure as a function of the modifier for a given stoichiometry. It should also be relevant to the glass formability of the corresponding melts and finds support in the devitrification data recently available for selected glasses (39,40).

4. INFRARED SPECTRA OF ALKALI-BORATE GLASSES

4.1. Compositional Dependence of the Glass Network Structure (0<x<0.73)

The infrared absorption spectra of lithium-borate glasses, obtained by Kramers-Kronig analysis of the reflectance spectra, are shown in Figures 8 and 9 . It is obvious that additions of Li_2O to B_2O_3 result in significant spectral changes, which illustrate the continuous structural variation of the borate network. The measured infrared spectra appear more complex than the Raman ones, due to the presence of broad and extensively overlapping bands. Nevertheless, three spectral regions can be distinguished in the mid-infrared : 1200-1450 cm^{-1} (B-O stretching vibrations of trigonal BO_3 units), 850-1200 cm^{-1} (B-O stretching vibrations of tetrahedral BO_4 units) and 600-800 cm^{-1} (originating from bending vibrations of the borate network) (4,17).

The first obvious effect of adding Li_2O to B_2O_3 is the growing of a multiple band (800-1200 cm^{-1}) , attributed to $B\emptyset_4^-$ absorptions. This envelope exhibits a maximum relative intensity for x=0.40, and then it decreases upon further increasing x. Such a behaviour is indicative of the initial creation of $B\emptyset_4^-$ tetrahedra-containing groups, followed by their subsequent destruction in favour of non-bridging oxygen-containing units (x>0.40). This is in accordance with the findings of NMR spectroscopy for this and similar glass systems (41).

Careful comparison of the spectra of Figures 8 and 9 with those of crystalline borate compounds of similar compositions (4,42) suggests that the initially created $B\emptyset_4^-$ tetrahedra are found in pentaborate (Fig.3.(2)) groups, which are then replaced by diborate arrangements (Fig.3(4)) with maximum concentration at x=0.40. The subsequent destruction of the latter groups is due to the creation of non-bridging oxygens as suggested by the appearance of the 1240 cm^{-1} band (x>0.40). This is a characteristic feature of the infrared spectrum of crystalline α-$Li_2O.B_2O_3$, known to consist of metaborate chains (Fig.3(6)) (42). In addition, the 1135 cm^{-1} band, developing at the high frequency side of the $B\emptyset_4^-$ absorption envelope, denotes the formation of pyroborate units.

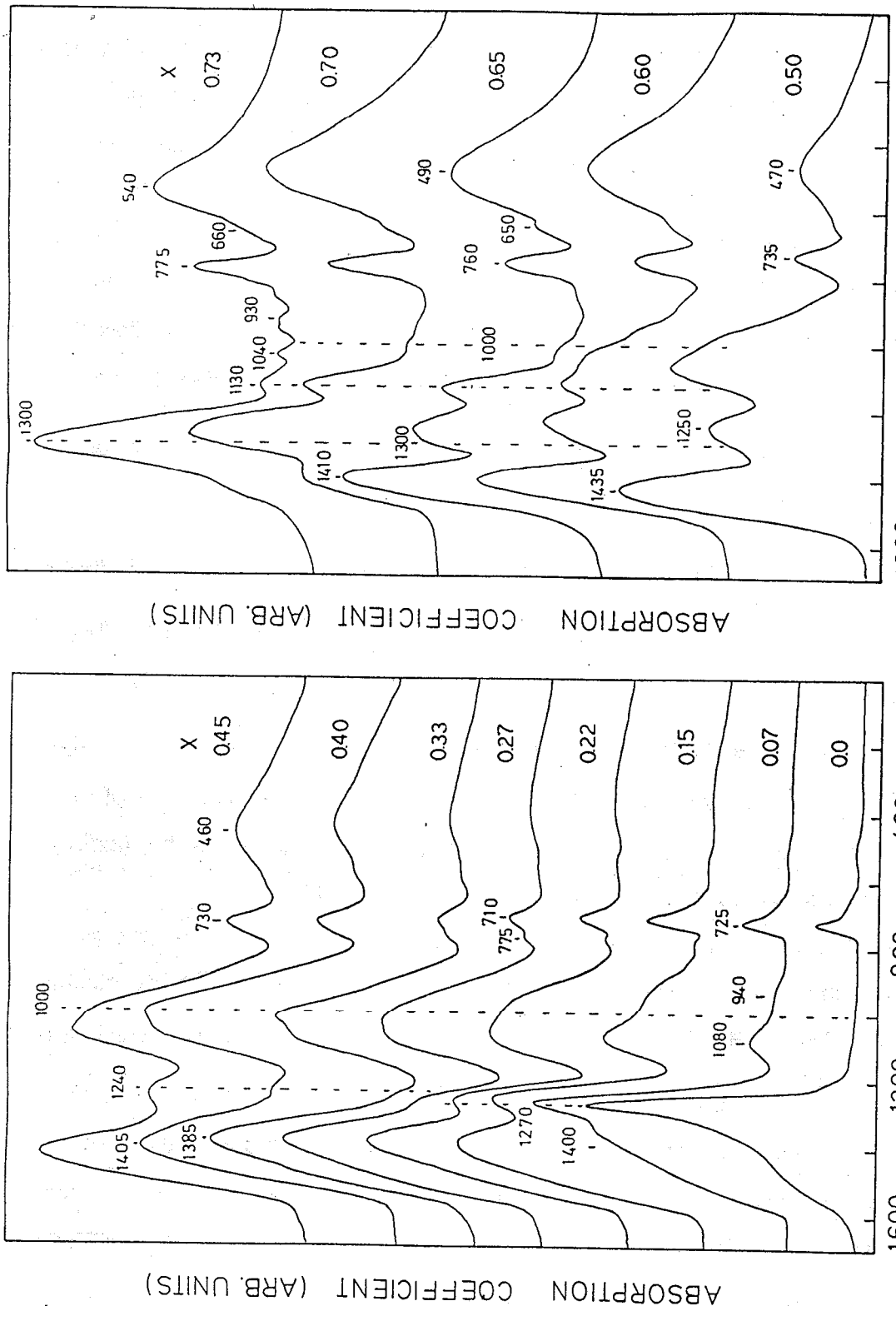

Figure 8. Infrared spectra of $xLi_2O.(1-x)B_2O_3$ glasses ($0 \leq x \leq 0.45$).

Figure 9. Infrared spectra of Li-borate glasses ($0.50 \leq x \leq 0.73$).

The dominant absorption of the x=0.73 glass spectrum is that at 1300 cm^{-1}, observed originally as a shoulder to the 1250 cm^{-1} band. Crystalline lithium orthoborate ($3Li_2O.B_2O_3$) gives its strongest absorption at this frequency, as a result of the infrared active asymmetric stretching vibration of BO_3^{3-} units (42). Thus, the borate network of the x=0.73 lithium glass appears to the built up mainly of orthoborate units and contains a minor concentration of pyroborates (1130 cm^{-1}) as well as groups with $B\emptyset_4^-$ tetrahedra (1040, 960 cm^{-1}). The second strongest feature of the mid infrared spectrum of this glass is that at 775 cm^{-1}, which can be assigned to the out-of-plane bending vibration of BO_3^{3-} units, while the in plane bending mode gives rise to the 650 cm^{-1} shoulder of the Li-motion band (34).

Detailed assignments of all infrared features requires careful deconvolution of the glass spectra and comparison with crystalline analogous compounds. While the details of the deconvolution can be found elsewhere (42), we present here the summarized results of this study (Figure 10) expressed as the relative concentration of various borate units as a function of Li_2O content. This enables the illustration of the network modification scenario upon increasing the amount of modifier oxide (Li_2O). Thus, the relative concentration of borate groups with $B\emptyset_4^-$ tetrahedra peaks at x=0.40, with obvious shoulders at x=0.20 and x=0.50, while metaborate chains and pyroborate units exhibit their maximum concentration of x=0.50 and x=0.65 respectively. The trigonal orthoborate units are the dominant species in glasses of very high Li_2O content.

The above modification pattern for lithium borate glasses is in general agreement with that deduced from the Raman studies of the same glasses. However, it is at pronounced variance with that found for Cs- and Rb-borate glasses, especially of high M_2O contents. This is presumably the manifestation of the "preference" of each alkali cation to specific borate units.

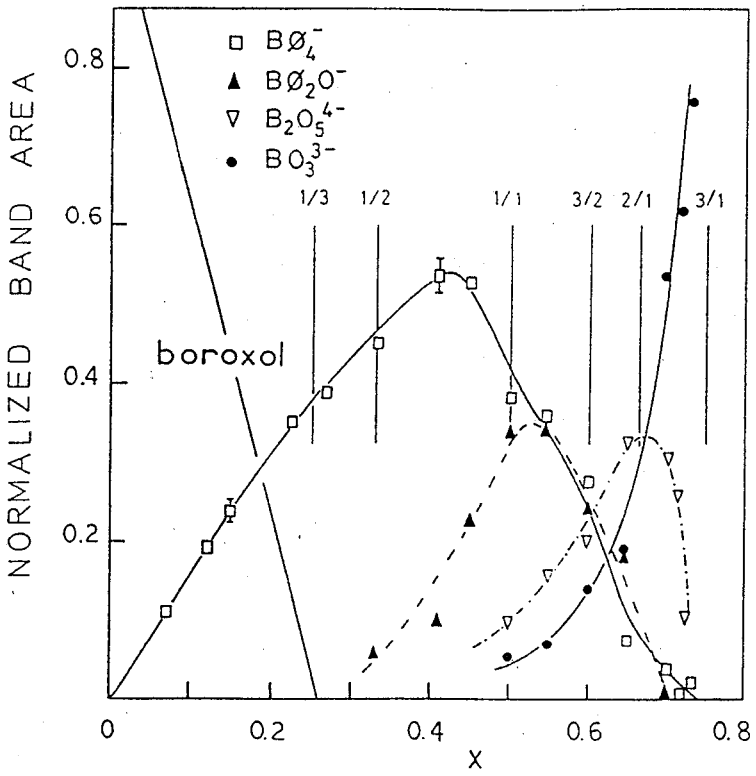

Figure 10. Normalized infrared band areas of borate units encountered in Li-borate glasses. $B\emptyset_4^-$ denotes borate groups containing boron-oxygen tetrahedra (Fig.3 (2,3,4,7)) and $B\emptyset_2O^-$ indicates metaborate chains. Vertical lines mark the stoichiometries of known crystalline Li-borate compounds. The composition dependence of boroxol rings has been determined from the Raman Spectra (17, 25).

4.2. Cation-Network Interactions

While the network vibrations contribute mostly to the mid-infrarted absorption profile, the alkali cation-site vibrational modes dominate the low frequency part of the spectrum (18). As shown in Figures 8,9, the absorption in the 50-600 cm^{-1} spectral region is progressively increasing with x and results into a broad and asymmetric band with both frequency at maximum and relative intensity increasing with Li_2O content. The large relative bandwidth of this feature has been associated with the broad distribution of similar Li^+-hosting sites in the glass (19). A Born-Mayer potential has been recently employed to model these cation-site interactions. For example, an analytical expression has been obtained con-

necting the characteristic cation vibrational frequency to the cation and anionic site parameters (19,43).

Careful deconvolution of the far-infrared absorption envelope has revealed the presence of the two Gaussian components in the majority of the glasses studied. These are marked as H and L in the representative spectra of Figure 11, and are taken to indicate distinct types of cation-hosting environments in glass (19,44). It is worth noting that the relative bandwidth of the low frequency component band (i.e. the ratio of the width at half maximum versus the frequency at maximum) is about twice as that of the high frequency component. This has been associated with a difference in the "amorphicity" of the two environments (42) and may be relevant to the recent views of glass formation and ionic transport (45).

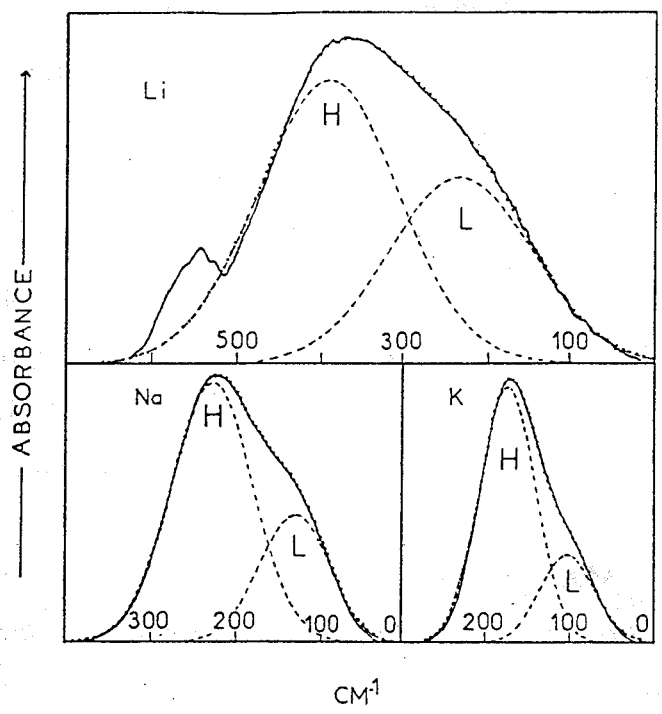

Figure 11. Representative deconvolution of far-infrared spectra of borate glasses containing 35 mol% alkali oxide.

5. CONCLUSIONS

Raman and infrared spectroscopic techniques are powerful in providing structural insight for borate glasses. The results presented in this report, together with the available literature, point to the strong dependence of the network modification scenario on the nature of the cationic modifier. It could have been expected that this cation dependence would be most obvious in glasses with high alkali contents. Indeed, this is now demostrated a least on a qualitative basis. The smallest alkali cations, Li^+ and Na^+, seem to favour the complete disruption of the borate network into isolated units, because of their high charge density. Correspondingly, the fraction of four-coordinated boron atoms, N_4, after going through a maximum at x=0.35, is progressively reduced smoothly towards a limiting value of zero as the glass composition approaches the orthoborate stoichiometry (x=0.75). To the contrary, the large and polarizable alkali cations (Rb^+, Cs^+) do not favour this reversal of boron-oxygen coordination from four to three. Instead, the N_4 value of the 75 mol% Cs_2O-glass is approaching unity due to the formation of tetracoordinated boron atoms with two non-bridging oxygens, which are not encountered in their Li- and Na-analogs.

These results are expected to trigger the investigation of high alkali content borates by NMR and other techniques. They also open the way for a detailed study of the devitrification mechanisms for these glasses, to confirm the nature of the high temperature equilibria thought to account for the diversity of the modification schemes. Much will be gained also in terms of understanding the glass formability of the corresponding borate melts, and the glass transport properties.

Acknowledgement : *Most results presented in this report are based on the research projects of a number of graduate students working in the glass group, at the National Hellenic Research Foundation.*

REFERENCES

1. D.L.Griscom in "Borate Glass:Structure, Properties and Applications", Eds. L.D.Pye, V.D.Frechette and N.J.Kreidl, New York, Plenum Press (1978) p.p. 11-149.

2. A.H.Silver and P.J.Bray, J.Chem.Phys. 29, 984 (1958)
3. P.J.Bray and J.G.O' Keefe, Phys.Chem.Glasses 4, 37 (1963)
4. J.Krogh Moe, Phys.Chem.Glasses, 6, 46 (1965)
5. W.L.Konijnendijk and J.M.Stevels, J.Non-Cryst.Solids, 18, 307 (1975)
6. H.L.Tuller, D.P.Button and D.R.Uhlmann, J.Non-Cryst.Solids, 40, 93 (1980)
7. A.Levasseur, M.Kbala, P.Hagenmüller, G.Couturier and Y.Danton, Solid State Ionics, 9-10, 1439 (1983)
8. Y.Ito, K.Miyauchi and T.Oi, J.Non-Cryst.Solids, 57, 389 (1983)
9. M.D.Ingram, Phys.Chem.Glasses, 28, 215 (1987)
10. H.L.Tuller and P.K.Moon, Mater.Sci. and Engineering, B1, 171 (1988)
11. C.Julien, M.Massot, P.Dzwonkowski, J.Y.Emery and M.Balkanski, Infrared Phys. 29, 769 (1989)
12. M.D.Ingram, M.A.Mackenzie, W.Müller and M.Torge, Solid State Ionics, in press, (presented at Hakone, Japan, Nov.1989)
13. J.Wong and C.A.Angell, "Glass Structure by Spectroscopy", Marcel Dekker, New York (1976)
14. W.L.Konijnendijk, Philips Res.Rep.Supl. No1 (1975)
15. J.T.Quan and C.E.Adams, J.Phys.Chem., 70, 340 (1966)
16. E.I.Kamitsos, M.A.Karakassides, G.D.Chryssikos, J.Phys.Chem., 91, 1073 (1987)
17. E.I.Kamitsos, M.A.Karakassides and G.D.Chryssikos, Phys.Chem.Glasses, 28, 203 (1987)
18. G.J.Exarhos and W.M.Risen, Jr., Chem.Phys.Lett, 10, 484 (1971)
19. E.I.Kamitsos, M.A.Karakassides and G.D.Chryssikos, J.Phys.Chem., 91, 5807 (1987)
20. N.F.Borrelli, B.D.McSwain and G.-J.Su, Phys.Chem.Glasses, 4, 11 (1963)
21. M.Irion, M.Couzi, A.Levasseur, J.M.Reau and J.C.Brethous, J.Solid State Chem. 31, 285 (1980)
22. M.Massot, C.Julien and M.Balkanski, Infrared Physics, 29, 775 (1989)
23. S.W.Martin and C.A.Angell, J.Non-Crystalline Solids, 66, 429 (1984)
24. M.Shibata, C.Sanchez, H.Patel, S.Feller, S.Stark, G.Sumcad and J.Kasper, J.Non-Cryst.Solids, 85, 29 (1986)
25. E.I.Kamitsos and M.A.Karakassides , Phys.Chem. Glasses, 30, 19 (1989)

26. G.D.Chryssikos, E.I.Kamitsos, A.P.Patsis and M.A.Karakassides, Mater.Sci. and Engineering B, in press (1990)
27. J.Goubeau and H.Keller, Z.Anorg.Allg.Chem. 272, 303 (1953)
28. L.A.Kristiansen and J.Krogh-Moe, Phys.Chem. Glasses, 9, 96 (1968)
29. F.L.Galeener, G.Lucovsky and J.C.Mikkelsen, Jr., Phys.Rev. B22, 3983 (1980)
30. C.F.Windisch and W.M.Risen, Jr., J.Non-Cryst.Solids, 48, 307 (1982)
31. P.A.V.Johnson, A.C.Wright and R.N.Sinclair, J.Non-Cryst.Solids, 50, 281 (1982)
32. A.C.Hannon, R.N.Sinclair, J.A.Blackman, A.C.Wright and F.L.Galeener, J.Non-Cryst.Solids, 106, 116 (1988)
33. T.W.Brill, Philips Res.Rep. Suppl., No1 (1975)
34. K.Nakamoto, "Infrared and Raman Spectra of Inorganic and Coordination Compounds", J.Wiley, New York, (1978)
35. J.B.Bates, M.H.Brooker, A.S.Quist and G.E.Boyd, J.Phys.Chem., 76, 1565 (1971)
36. E.I.Kamitsos, M.A.Karakassides and A.P.Patsis, J.Non-Cryst.Solids, 111, 252 (1989)
37. E.I.Kamitsos, M.A.Karakassides and G.D.Chryssikos, Phys.Chem.Glasses, 30, 229 (1989)
38. G.D.Chryssikos, E.I.Kamitsos and M.A.Karakassides, Phys.Chem.Glasses, 31, 109 (1990)
39. E.I.Kamitsos, M.A.Karakassides, A.P.Patsis and G.D.Chryssikos, J.Non-Cryst.Solids, 116 , 115 (1990).
40. G.D.Chryssikos, E.I.Kamitsos, A.P.Patsis, M.S.Bitsis and M.A.Karakassides, J.Non-Cryst. Solids, in press (1991)
41. Y.H.Yun and P.J.Bray, J.Non-Cryst.Solids, 44, 227 (1981)
42. E.I.Kamitsos, A.P.Patsis, M.A.Karakassides and G.D.Chryssikos, J.Non-Cryst. Solids, in press (1991).
43. E.I.Kamitsos, J.Phys. Chem. 93, 1604 (1989)
44. E.I.Kamitsos, M.A.Karakassides and G.D.Chryssikos, Solid State Ionics, 28-30, 687 (1988)
45. M.D.Ingram, Phil. Mag. B60, 729 (1989)